
Since January 2020 Elsevier has created a COVID-19 resource centre with free information in English and Mandarin on the novel coronavirus COVID-19. The COVID-19 resource centre is hosted on Elsevier Connect, the company's public news and information website.

Mathematical Biosciences 337 (2021) 108621

Contents lists available at ScienceDirect

Mathematical Biosciences

journal homepage: www.elsevier.com/locate/mbs

Original Research Article

# Optimal allocation of limited vaccine to control an infectious disease: Simple analytical conditions☆

Isabelle J. Rao *, Margaret L. Brandeau

*Department of Management Science and Engineering, Stanford University, Stanford, CA, United States of America*

ARTICLE INFO

*Keywords:*
Vaccine allocation
Optimization
COVID-19
Dynamic disease model
Epidemic control
Health policy

ABSTRACT

When allocating limited vaccines to control an infectious disease, policy makers frequently have goals relating to individual health benefits (e.g., reduced morbidity and mortality) as well as population-level health benefits (e.g., reduced transmission and possible disease eradication). We consider the optimal allocation of a limited supply of a preventive vaccine to control an infectious disease, and four different allocation objectives: minimize new infections, deaths, life years lost, or quality-adjusted life years (QALYs) lost due to death. We consider an SIR model with $n$ interacting populations, and a single allocation of vaccine at time 0. We approximate the model dynamics to develop simple analytical conditions characterizing the optimal vaccine allocation for each objective. We instantiate the model for an epidemic similar to COVID-19 and consider $n = 2$ population groups: one group (individuals under age 65) with high transmission but low mortality and the other group (individuals age 65 or older) with low transmission but high mortality. We find that it is optimal to vaccinate younger individuals to minimize new infections, whereas it is optimal to vaccinate older individuals to minimize deaths, life years lost, or QALYs lost due to death. Numerical simulations show that the allocations resulting from our conditions match those found using much more computationally expensive algorithms such as exhaustive search. Sensitivity analysis on key parameters indicates that the optimal allocation is robust to changes in parameter values. The simple conditions we develop provide a useful means of informing vaccine allocation decisions for communicable diseases.

## 1. Background

When allocating limited vaccines to control an infectious disease, policy makers frequently have goals relating to individual health benefits (e.g., reduced morbidity and mortality) as well as population-level health benefits (e.g., reduced transmission and possible disease eradication). For example, a recent report from the National Academy of Sciences, Engineering and Medicine on equitable allocation of vaccine for SARS-CoV-2, the virus that causes COVID-19 infection, states that "The goal of the committee's framework for equitable allocation of COVID-19 vaccine is to reduce morbidity, mortality, and negative societal impact due to the transmission of the novel coronavirus" [1]. Such goals are not necessarily compatible, however, as individuals who are most likely to die from a disease may not be most likely to transmit the disease.

Different approaches to the vaccine allocation problem have been proposed. For a general infectious disease, some studies formulate the problem as a mixed-integer or linear programming problem with the objective of minimizing the number or cost of vaccines such that the reproductive ratio $R_0$ is below 1 [2–4]. One study considers a two-period problem with the goal of allocating a fixed number of vaccine doses to minimize the fraction of people who become infected [5]. Other studies use an optimal control formulation to determine the continuous allocation of vaccine with the goal of minimizing vaccination cost plus the cost of infection [6,7]. Many vaccine allocation studies use compartmental epidemic models and assume homogeneous mixing. One study shows by introducing variability in the transmission rates between population groups that eradication of an epidemic is possible with fewer vaccinations than under the homogeneous assumption [8]. More broadly, another study develops an SI model to allocate resources among a set of interventions to control an epidemic in non-interacting population groups [9]. The authors use Taylor series expansions to approximate the objective function and show that some formulations of the model are equivalent to a knapsack problem.

A number of vaccine allocation studies have focused on seasonal influenza. Some researchers use age-structured compartmental models with numerical simulations to evaluate the impact of different vaccination strategies [10,11]. One study uses numerical optimization to determine the optimal allocation of influenza vaccine between low-

☆ This work was supported by Grant R37-DA15612 from the National Institute on Drug Abuse.
* Correspondence to: Huang Engineering Center, 475 Via Ortega, Stanford, CA 94305, United States of America.
*E-mail addresses:* isarao@stanford.edu (I.J. Rao), brandeau@stanford.edu (M.L. Brandeau).

https://doi.org/10.1016/j.mbs.2021.108621
Received 24 February 2021; Received in revised form 23 April 2021; Accepted 25 April 2021
Available online 27 April 2021

and high-risk children and adults at different time points to minimize deaths or hospitalizations [12] and another study considers the optimal influenza vaccination policy for five different outcomes: deaths, infections, years of life lost, contingent value, and economic loss [13]. Both studies find that population age structure is an important factor in determining the optimal influenza vaccine distribution.

Recent studies have examined optimal vaccination policies for COVID-19. One study considers the choice between vaccinating high-risk individuals in low-exposure occupations versus low-risk individuals in high-exposure occupations, with the goal of minimizing the cost of infections plus economic losses [14]. The authors find that the optimal vaccine allocation should prioritize age-based fatality rates rather than occupation-based infection rates. Another study uses an age-stratified model to determine the optimal vaccine allocation for four different outcomes: deaths, symptomatic infections, and maximum non-ICU and ICU hospitalizations [15]. The authors find that when vaccine coverage can reach at most 60% of the population, younger age groups should be vaccinated to minimize symptomatic infections or non-ICU hospitalizations, whereas older age groups should be vaccinated to minimize deaths or ICU hospitalizations; for coverage levels above 60%, the optimal strategy for all four objectives is to vaccinate high-transmission groups. One study uses a multi-period age-stratified model with the goal of minimizing the number of deaths or confirmed cases [16]. The authors show that, for static policies, vaccinating older groups averts more deaths, whereas vaccinating younger groups averts more infections; for dynamic policies, older people should be vaccinated first, followed by younger people.

In this paper we consider the optimal allocation of a limited supply of a preventive vaccine to control an infectious disease. We explore the impact of four different objectives: minimize new infections, deaths, life years lost, or quality-adjusted life years (QALYs) lost due to death. We consider an SIR model with $n$ interacting populations, and a single allocation of vaccine at time 0. We approximate the model dynamics to develop simple analytical conditions characterizing the optimal vaccine allocation for each objective. We instantiate the model for an epidemic similar to the COVID-19 epidemic in New York State, both during an initial outbreak and during a resurgence, and consider $n = 2$ population groups: one group (individuals under age 65) with high transmission but low mortality and the other group (individuals age 65 or older) with low transmission but high mortality. We determine the optimal vaccine allocation for the different objectives, and assess the quality of solutions from the approximated model.

## 2. Framework

### 2.1. SIR model with vaccination

We develop an SIR model of a population with $n \geq 2$ interacting groups in which an infectious disease is spreading (Fig. 1). Individuals in each group $i$ can be susceptible ($S_i$), infected ($I_i$), recovered ($R_i$), or dead ($D_i$). Individuals in group $i$ can acquire infection from contact with individuals in their own population group (at rate $\beta_{ii}$) or another population group $j$ (at rate $\beta_{ij}$). Infected individuals in group $i$ either recover (at rate $\gamma_i$) or die (at rate $\mu_i$). We consider a relatively short time horizon and thus do not include births, non-infection-related deaths, or other forms of entry into and exit from the population.

The compartmental model is governed by the following differential equations:

$$\begin{aligned}
\frac{\mathrm{d}S_i}{\mathrm{d}t} &= -S_i\Big(\sum_{j=1}^{n}\beta_{ij}I_j\Big) && \forall i \in [\![1,n]\!] \\
\frac{\mathrm{d}I_i}{\mathrm{d}t} &= S_i\Big(\sum_{j=1}^{n}\beta_{ij}I_j\Big) - (\gamma_i+\mu_i)I_i && \forall i \in [\![1,n]\!] \\
\frac{\mathrm{d}R_i}{\mathrm{d}t} &= \gamma_i I_i && \forall i \in [\![1,n]\!] \\
\frac{\mathrm{d}D_i}{\mathrm{d}t} &= \mu_i I_i && \forall i \in [\![1,n]\!]
\end{aligned} \tag{1}$$

We assume that a preventive vaccine with effectiveness $\eta > 0$ is available and that vaccination of susceptible individuals moves them to a recovered health state. Vaccination does not affect the transmission rates between infected and unvaccinated individuals ($\beta_{i,j}$) nor the recovery rates of infected individuals ($\gamma_i$). We let $P$ denote the population size, and $v = (v_1, v_2, \ldots, v_n) \in \mathbb{R}^n$ denote the proportion of individuals vaccinated. More specifically, $v_i$ is the proportion of the entire population that is vaccinated and belongs to group $i$. We further assume that a limited number of vaccines, $N < P$, are available to be distributed at time 0 such that $\sum_i v_i \leq \frac{N}{P}$.

We denote by $S_i(0)$, $I_i(0)$, $R_i(0)$ and $D_i(0)$ the proportion of the entire population in each compartment at time 0 without vaccination. We let $S_i(v;t)$, $I_i(v;t)$, $R_i(v;t)$, and $D_i(v;t)$ be the proportion of individuals in each compartment at time $t$ in the presence of vaccination $v$. By definition, we have:

$$\sum_{i=1}^{n} S_i(v;t) + I_i(v;t) + R_i(v;t) + D_i(v;t) = 1, \quad \forall v, t$$

Since vaccination only impacts the initial conditions, we have $\forall i \in [\![1,n]\!]$

$$\begin{aligned}
S_i(v;0) &= S_i(0) - \eta v_i \\
I_i(v;0) &= I_i(0) \\
R_i(v;0) &= R_i(0) + \eta v_i \\
D_i(v;0) &= D_i(0)
\end{aligned} \tag{2}$$

The problem of optimal vaccine allocation can be expressed as follows, where $f(v)$ denotes the objective to be optimized:

$$\begin{aligned}
\underset{v}{\text{minimize}} \quad & f(v) \\
\text{subject to} \quad & \sum_{i=1}^{n} v_i \leq \frac{N}{P} \\
& v_i \leq S_i(0) && \forall i \in [\![1,n]\!] \\
& v_i \geq 0 && \forall i \in [\![1,n]\!]
\end{aligned} \tag{3}$$

The constraints in the above formulation provide limits on the total fraction of the population that can be vaccinated and on the total fraction of each population group that can be vaccinated. If desired, an equity constraint can be added:

$$v_i \geq m_i, \quad \forall i \in [\![1,n]\!]$$

where $m_i$ is the minimum fraction of the population in group $i$ that must be vaccinated. In this case, we consider $v' = (v'_1, v'_2, \ldots, v'_n) = (v_1 - m_1, v_2 - m_2, \ldots, v_n - m_n)$ as our decision variable with the constraints $v'_i \geq 0, \forall i \in [\![1,n]\!]$.

### 2.2. Objective functions

We consider four different objectives for the vaccine allocation problem, measured over a time horizon of length $T$.

**Minimize new infections.** The objective of minimizing the total number of new infections can be written as

$$f(v) = INF(v;T) = \sum_{i=1}^{n}\big(I_i(v;T) + R_i(v;T) - \eta v_i + D_i(v;T)\big). \tag{4}$$

Note that we subtract the proportion of recovered individuals in each group $i$, $R_i(v;T)$, by $\eta v_i$ because vaccination moves a proportion $\eta v_i$ of individuals to the recovered state as can be seen in (2), but these individuals were never infected.

**Minimize deaths.** The objective of minimizing the total number of deaths can be written as

$$f(v) = D(v;T) = \sum_{i=1}^{n} D_i(v;T). \tag{5}$$

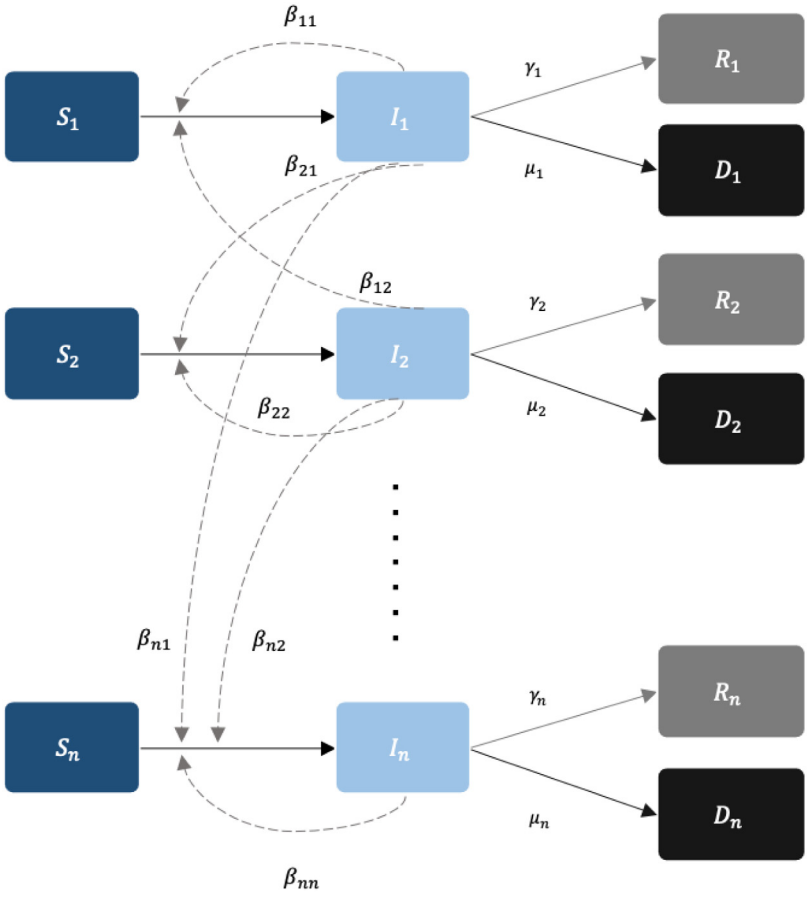


**Fig. 1.** Dynamic compartmental model.

**Minimize life years lost.** The objective of minimizing life years lost can be written as

$$f(v) = LY(v;T) = \sum_{i=1}^{n} L_i D_i(v;T) \tag{6}$$

where $L_i$ is the average expected life years lost due to death of an individual in group $i$.

**Minimize QALYs lost due to death.** The objective of minimizing QALYs lost due to death can be written as

$$f(v) = QALY(v;T) = \sum_{i=1}^{n} q_i L_i D_i(v;T) \tag{7}$$

where $q_i$ is the average QALY multiplier for individuals in group $i$. Note that (7) does not include QALY losses that occur during the period when an individual is infected.

## 3. Simple conditions for vaccine allocation

### 3.1. Taylor series expansions

Because an analytical solution for an SIR model with $n$ interacting populations would be difficult or even impossible to derive, we approximate the disease dynamics at time $T$ using first- and second-order Taylor series expansions:

$$\begin{aligned} x(v;t) &\simeq x(v;0) + \frac{\mathrm{d}x}{\mathrm{d}t}(v;0)t, \quad \text{for } x \in \{I_i, R_i, D_i\}, t \geq 0 \\ x(v;t) &\simeq x(v;0) + \frac{\mathrm{d}x}{\mathrm{d}t}(v;0)t + \frac{\mathrm{d}^2x}{\mathrm{d}t^2}(v;0)\frac{t^2}{2}, \quad \text{for } x \in \{D_i\}, t \geq 0 \end{aligned} \tag{8}$$

A similar approach was used by Zaric and Brandeau [9] for an SI model, under the assumption that no sufficient contacts occur across population groups. We extend this approach to an SIR model with $n$ groups, and allow cross-infection between groups: $\beta_{ij} \neq 0$ for $i \neq j$.

For the objective of minimizing infections, we use first-order approximations. Combining Eqs. (1), (2) and (8), we have the following approximate expressions for compartment sizes at $t = T$:

$$\begin{aligned} I_i(v;T) &\simeq I_i(0) + (S_i(0) - \eta v_i)\Big(\sum_{j=1}^{n} \beta_{ij} I_j(0)\Big)T - (\gamma_i + \mu_i) I_i(0) T \\ R_i(v;T) &\simeq R_i(0) + \eta v_i + \gamma_i I_i(0) T \\ D_i(v;T) &\simeq D_i(0) + \mu_i I_i(0) T \end{aligned} \tag{9}$$

The above approximations of $I_i$ and $R_i$ are linear functions of $v$. As we will show in Section 3.2, this allows us to derive an analytical solution to the optimal vaccine allocation problem when considering the objective of minimizing infections.

For the objectives of minimizing deaths, life years lost, and QALYs lost due to death, we use a second-order approximation to estimate $D_i(v;T)$:

$$\begin{aligned} D_i(v;T) \simeq \quad & D_i(0) + \mu_i I_i(0) T \\ & + \mu_i \Big((S_i(0) - \eta v_i)\Big(\sum_{j=1}^{n} \beta_{ij} I_j(0)\Big) - (\gamma_i + \mu_i) I_i(0)\Big)\frac{T^2}{2}. \end{aligned} \tag{10}$$

The above approximation of $D_i$ is a linear function of $v$. This allows us to derive an analytical solution for the optimal vaccination problem when considering the objective of minimizing deaths, life years lost, or QALYs lost due to death, as we will show in Section 3.2.

These approximations have limitations and should be handled with care in order for the resulting model to be realistic. Specifically, with sufficient levels of vaccines ($v$), the first-order approximation of $I_i$ can be negative, and the second-order approximation of $D_i$ can be

decreasing. In particular,

$$v_i \geq \frac{1}{\eta}\Big(S_i(0) - \frac{(\gamma_i+\mu_i)I_i(0)T - I_i(0)}{(\sum_{j=1}^{n}\beta_{ij}I_j(0))T}\Big) = \alpha_i(T)$$
$$\implies \begin{cases} I_i(v;T) \leq 0, & i \in [\![1,n]\!]. \\ \frac{dD_i}{dt}(v;T) \leq 0, & i \in [\![1,n]\!]. \end{cases}$$

Since $t \mapsto \alpha_i(t)$ is a decreasing function of $t$, we have $\alpha_i(T) \leq \alpha_i(t), \forall t \leq T$ such that

$$v_i \leq \alpha_i(T) \implies \begin{cases} I_i(v,t) \geq 0, & \forall t \leq T \\ \frac{dD_i}{dt}(v,t) \geq 0, & \forall t \leq T. \end{cases}$$

Let $\tau(T) = \min_i\{\alpha_i(T)\}$. For the purpose of this analysis, we assume that the number of available vaccines for time horizon $T$ is less than $\tau(T)$; thus, our approximation of $INF(v;T)$ is always positive and our approximations of $D(v;T)$, $LY(v;T)$, and $QALY(v;T)$ are always non-decreasing over the time period considered.

### 3.2. Optimal solution to the allocation problem

**Minimize new infections.** We approximate the objective (4) using (9):

$$\mathrm{INF}(v;T) \simeq \sum_i \big(I_i(0) + R_i(0) + D_i(0)\big) + \sum_i (S_i(0) - \eta v_i)\Big(\sum_j \beta_{ij} I_j(0)\Big)T.$$

Dropping the constant terms, and since $\eta > 0$, the objective function for the optimization problem (3) is:

$$f(v) = -\sum_i v_i\Big(\sum_j \beta_{ij} I_j(0)\Big). \tag{11}$$

Since (11) is a linear function of $v$, the optimization problem (3) becomes a knapsack problem, with weights $w_i = 1\ \forall i$, and value equal to the initial force of infection: $p_i = \sum_j \beta_{ij} I_j(0)\ \ \forall i$. The optimal solution is to vaccinate groups in decreasing order of the coefficient $p_i/w_i$. Specifically, we order the groups by decreasing order of their initial force of infection, and let $k = \max\{k' | 1 \leq k' \leq n, \sum_{i=1}^{k'} S_i(0) \leq \frac{N}{P}\}$. The optimal solution is

$$v^* = \begin{bmatrix} v_1^* \\ \vdots \\ v_k^* \\ v_{k+1}^* \\ v_{k+2}^* \\ \vdots \\ v_n^* \end{bmatrix} = \begin{bmatrix} S_1(0) \\ \vdots \\ S_k(0) \\ \frac{N}{P} - \sum_{i=1}^{k} S_i(0) \\ 0 \\ \vdots \\ 0 \end{bmatrix}. \tag{12}$$

In other words, if

$$\sum_j \beta_{ij} I_j(0) \geq \sum_j \beta_{lj} I_j(0), \tag{13}$$

then allocating all vaccine to group $i$ until all susceptible individuals in group $i$ are vaccinated averts more estimated infections than does allocating any vaccines to group $l$.

**Minimize deaths.** We proceed in a similar manner for the objective of minimizing deaths. We approximate the objective (5) using (10) as

$$D(v;T) \simeq \sum_i \big(D_i(0) + \mu_i I_i(0)T\big) + \frac{T^2}{2}\sum_i \mu_i\big[(S_i(0) - \eta v_i)\Big(\sum_j \beta_{ij} I_j(0)\Big) - (\gamma_i + \mu_i)I_i(0)\big].$$

Dropping the constant terms, and since $\eta > 0$, the objective function becomes:

$$f(v) = -\sum_i v_i\big(\mu_i \sum_j \beta_{ij} I_j(0)\big). \tag{14}$$

This objective is again a linear function of $v$, and we solve a knapsack problem. Ordering the groups in decreasing order of their initial force of infection multiplied by the mortality rate, $\mu_i \sum_j \beta_{ij} I_j(0)$, the optimal solution is given by (12). If

$$\mu_i \sum_j \beta_{ij} I_j(0) \geq \mu_l \sum_j \beta_{lj} I_j(0), \tag{15}$$

then it is optimal to allocate vaccines to group $i$ before group $l$ in order to minimize deaths. Condition (15) is similar to that for the case of minimizing new infections (13), but now weighted by the mortality rates $\mu_i$.

**Minimize life years lost and QALYs lost.** The functions $D$, $LY$ and $QALY$ are weighted sums of $D_i$, with the weights being 1, $L_i$ and $q_i L_i$, respectively. Therefore, the solutions to minimizing life years lost and QALYs lost follow directly from the solution to minimizing deaths. Approximating the objectives (6) and (7) using (10), we find that the objective functions are linear functions of $v$ for both problems so we have a knapsack problem as before. The weights $w_i$ are still equal to one, and the values $p_i$ when minimizing life years lost and QALYs lost are similar to the case of minimizing deaths, but additionally weighted by the average expected life years lost $L_i$, and the average expected QALYs lost due to death $q_i L_i$, respectively.

Table 1 summarizes the coefficient $p_i/w_i$ of the knapsack problem for each of the four objectives. For each objective, it is optimal to vaccinate the groups in decreasing order of this coefficient; that is, if $p_i/w_i \geq p_l/w_l$, then it is optimal to vaccinate group $i$ before group $l$.

The conditions indicate that it is optimal to allocate the vaccines to one group until every individual in this group is vaccinated before allocating any vaccines to the remaining groups. The group that receives the vaccines first depends, respectively, on the force of infection ($\sum_j \beta_{ij} I_j(0)$), or the force of infection multiplied by the mortality rate ($\mu_i$), the expected life years lost ($L_i$), or the QALYs lost due to death ($q_i L_i$).

**Table 1**
Coefficients of the knapsack problem for the four objective functions.

| Objective | $p_i/w_i$ |
|---|---|
| Minimize infections | $\sum_j \beta_{ij} I_j(0)$ |
| Minimize deaths | $\mu_i \sum_j \beta_{ij} I_j(0)$ |
| Minimize life years lost | $L_i \mu_i \sum_j \beta_{ij} I_j(0)$ |
| Minimize QALYs lost | $q_i L_i \mu_i \sum_j \beta_{ij} I_j(0)$ |

## 4. Example: Vaccination against COVID-19

### 4.1. Model instantiation

We illustrate our ideas using the example of COVID-19 with two groups ($n = 2$). We assume that group 1 consists of individuals under age 65 and group 2 consists of individuals 65 years or older. To instantiate our model we use data that includes daily confirmed cases and deaths for New York state [17], with values for other model parameters drawn from the literature and public sources (Table 2). We assume that all individuals in group 1 have a QALY multiplier of 1. Using [18–20] we estimate QALYs lost due to death ($q_i L_i$) for both groups.

We compute the transition rates as follows:

$$d_1 = d_m + \alpha_1 d_s, \qquad \mu_1 = \frac{\xi_1}{d_1}, \qquad \gamma_1 = \frac{1}{d_1} - \mu_1$$
$$d_2 = d_m + \alpha_2 d_s, \qquad \mu_2 = \frac{\xi_2}{d_2}, \qquad \gamma_2 = \frac{1}{d_2} - \mu_2$$

The average duration of infection for an individual in group $i$ is the sum of the average duration of a mild infection, plus the average duration of a severe infection multiplied by the fraction of infections in group $i$ that are severe. The rate at which an individual in group $i$ leaves the infected compartment is $\frac{1}{d_i}$. Given that only a fraction $\xi_i$ of infected individuals die, the transition rate from infected to dead ($\mu_i$) is simply the product of $\xi_i$ and $\frac{1}{d_i}$. The remaining fraction $1 - \xi_i$ of the infected individuals

**Table 2**
Values and sources for model parameters.

| Parameter | Description | Value | Source |
|---|---|---|---|
| $f_1$ | Fraction of individuals <65 years old | 0.84 | [18] |
| $f_2$ | Fraction of individuals ≥65 years old | 0.16 | [18] |
| $d_m$ | Average duration of mild infection (days) | 11 | [21–24] |
| $d_s$ | Average duration of severe infection (days) | 8 | [25,26] |
| $\alpha_1$ | Fraction of infections that become severe for individuals <65 years old | 0.21 | [18,27] |
| $\alpha_2$ | Fraction of infections that become severe for individuals ≥65 years old | 0.46 | [18,27] |
| $d_1$ | Average duration of infection for individuals <65 years old (days) | 12.68 | Calculated |
| $d_2$ | Average duration of infection for individuals ≥65 years old (days) | 14.68 | Calculated |
| $\xi_1$ | Infected fatality ratio for individuals <65 years old | 0.00153 | [18,28] |
| $\xi_2$ | Infected fatality ratio for individuals ≥65 years old | 0.0675 | [18,28] |
| $\mu_1$ | Daily death rate for individuals <65 years old | 0.00012 | Calculated |
| $\mu_2$ | Daily death rate for individuals ≥65 years old | 0.00460 | Calculated |
| $\gamma_1$ | Daily rate at which individuals <65 years old recover and become immune | 0.079 | Calculated |
| $\gamma_2$ | Daily rate at which individuals ≥65 years old recover and become immune | 0.064 | Calculated |
| $\eta$ | Vaccine effectiveness | 0.90 | [29] |
| $L_1$ | Expected life years lost for individuals <65 years old | 46 | [18,19] |
| $L_2$ | Expected life years lost for individuals ≥65 years old | 13 | [18,19] |
| $q_1 L_1$ | Quality-adjusted expected life years lost for individuals <65 years old | 34.47 | [18–20] |
| $q_2 L_2$ | Quality-adjusted expected life years lost for individuals ≥65 years old | 6.96 | [18–20] |

recovers, and thus the transition rate from infected to recovered ($\gamma_i$) is equal to $\frac{1-\xi_i}{d_i} = \frac{1}{d_i} - \mu_i$.

We use model calibration to determine the transmission rate parameters $\beta_{11}$, $\beta_{12}$, $\beta_{21}$ and $\beta_{22}$, and the initial total number of infected individuals, $I(0) = I_1(0) + I_2(0)$. We assume that $\beta_{12} < \beta_{21}$, and that the distribution of cases initially is consistent with the age distribution, such that $I_1(0) = f_1 I(0)$ and $I_2(0) = f_2 I(0)$. Since several studies have shown that the total number of cases could be many times higher than the number of confirmed cases [30,31], we calibrate to a 7-day rolling average of reported deaths from March 1 to April 4, 2020 (Fig. 2(a)) and compare our model projections to multiples of a 7-day rolling average of new confirmed cases (Fig. 2(b)). We calibrate to daily deaths only up until April 4 since all non-essential statewide businesses closed in New York state beginning on March 22 [32], and we want to capture the trend of the epidemic during the initial outbreak, before any interventions took place.

We use Latin Hypercube Sampling for calibration, randomly sampling each parameter from a range of values [33]. We measure goodness of fit using the sum of squared errors. The calibrated parameter values are:

$$\beta_{11} = 0.403$$
$$\beta_{12} = 0.071$$
$$\beta_{21} = 0.154$$
$$\beta_{22} = 0.613$$
$$I(0) = 4.97 \times 10^{-6}$$
$$I_1(0) = 4.15 \times 10^{-6}$$
$$I_2(0) = 8.19 \times 10^{-7}$$

The resulting $R_0$ value is 4.31, which is consistent with other sources such as [34–37] that aim to estimate $R_0$ while taking into account not only confirmed cases but also extrapolating to unconfirmed cases.

Fig. 3 compares the calibrated model's output to the New York state data on deaths and confirmed cases. The model output closely matches the calibration target of reported deaths (Fig. 3(a)). The model's projected total number of infected individuals is 5 to 10 times higher than daily confirmed cases in New York state (Fig. 3(b)), which is consistent with studies such as [30] and [31] that suggest that the total number of people infected is 5–10 times the number of confirmed cases due to a large population of asymptomatic individuals and untested individuals.

We initialize the model with an estimate of the proportion of individuals in each compartment on November 5, 2020 in the United States [38], and using the transmission rates as calculated above. We assume that the distribution of the population in each compartment is consistent with the age distribution; that is, $I_1(0) = (.84)(I_1(0) + I_2(0))$ and $I_2(0) = (.16)(I_1(0)+I_2(0))$ (and similarly for $S$, $R$, and $D$). From [38] we have

$$I(0) = I_1(0) + I_2(0) = 1\%$$
$$R(0) = R_1(0) + R_2(0) = 2\%$$
$$D(0) = D_1(0) + D_2(0) = 0.1\%$$

We then deduce $S(0)$ given that $S(0) + I(0) + R(0) + D(0) = 1$. As there is uncertainty about the number of COVID-19 cases, we also consider scenarios where there are two, five, and ten times [39] as many infected and recovered individuals as reported (Supplemental Table A.1).

Since many measures have been put in place to prevent the spread of the epidemic (e.g., masks, shelter-in-place orders), for each scenario we also consider the case where transmission rates are halved compared to the initial outbreak due to these measures [40,41]. We will refer to these measures collectively as social distancing. Across all scenarios considered, with and without social distancing, we find that the basic reproductive number ranges from 1.5 to 4.2 (Supplemental Table A.2).

### 4.2. Optimal vaccine allocation

We consider three time horizons over which the vaccination objectives are measured: $T = 30, 90, 180$ days. We assume that a vaccine with effectiveness $\eta = 0.90$ is available [29]. Using the calibrated parameters, we determine $\tau(T)$, which is the maximum proportion of the population vaccinated that we can consider given our approximation (9) of the epidemic dynamics (Table 3).

From the optimality conditions (Table 1), we define

$$\begin{aligned} C_I &= \beta_{11} I_1(0) + \beta_{12} I_2(0) - (\beta_{21} I_1(0) + \beta_{22} I_2(0)) \\ C_D &= \mu_1(\beta_{11} I_1(0) + \beta_{12} I_2(0)) - \mu_2(\beta_{21} I_1(0) + \beta_{22} I_2(0)) \\ C_{LY} &= L_1\mu_1(\beta_{11} I_1(0) + \beta_{12} I_2(0)) - L_2\mu_2(\beta_{21} I_1(0) + \beta_{22} I_2(0)) \\ C_{QALY} &= q_1 L_1 \mu_1(\beta_{11} I_1(0) + \beta_{12} I_2(0)) - q_2 L_2 \mu_2(\beta_{21} I_1(0) + \beta_{22} I_2(0)) \end{aligned} \tag{16}$$

We calculate the values of $C_I, C_D, C_{LY}$ and $C_{QALY}$ with the calibrated parameters for each scenario (Supplemental Table A.3) to determine which group to vaccinate given the objective function considered. For example, if $C_I > 0$, then it is optimal to vaccinate group 1 rather than group 2 in order to minimize new infections.

Table 4 shows the optimal allocation for each objective function and scenario. The allocations varied for the different objectives, but did not vary by scenario. To minimize new infections it is always better to vaccinate individuals under 65 years old (group 1). Because there are more susceptible individuals under 65 years old than 65 years or older, and individuals in the younger group have a higher cross-transmission rate than individuals in the older group ($\beta_{21} > \beta_{12}$), vaccinating younger individuals averts more infections. However, in order to minimize

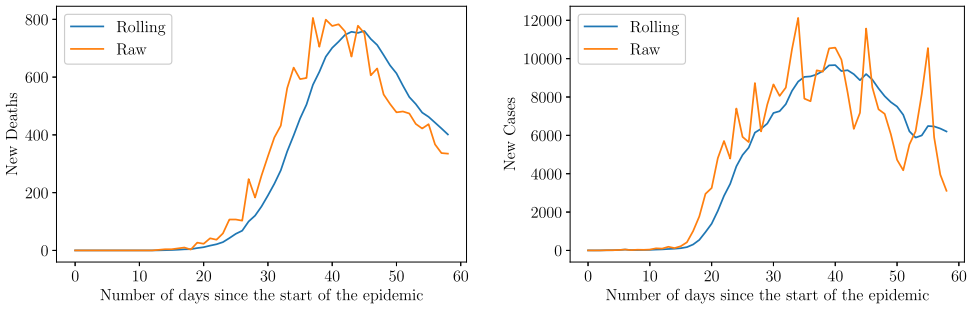


(a) New daily confirmed deaths (b) New daily confirmed cases

**Fig. 2.** New daily confirmed COVID-19 deaths and cases in New York state beginning from March 1: raw numbers and 7-day rolling average.

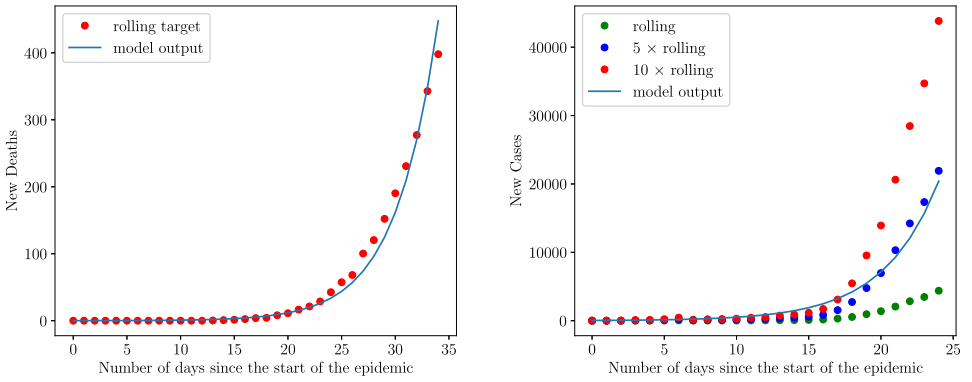


(a) New daily confirmed deaths (b) Multiples of new daily confirmed cases

**Fig. 3.** Calibrated model's daily number of deaths, and multiples of daily confirmed cases compared to reported values (7-day rolling averages) for New York state.

**Table 3**
Maximum proportion of the population that we consider vaccinating for each time horizon ($T = 30, 90, 180$ days) and epidemic scenario, and with or without social distancing. Scenario 1 assumes that the total number of initial infections equals the number of reported cases. Scenarios 2, 3, and 4 assume, respectively, that the total number of initial infections equals two, five, and ten times the number of reported cases.

| | | Scenario 1 | Scenario 2 | Scenario 3 | Scenario 4 |
|---|---|---|---|---|---|
| No social distancing | $T = 30$ days | 15.0% | 14.4% | 12.8% | 10.0% |
| | $T = 90$ days | 13.2% | 12.6% | 11.0% | 8.2% |
| | $T = 180$ days | 12.7% | 12.2% | 10.5% | 7.8% |
| Social distancing | $T = 30$ days | 12.2% | 11.6% | 10.0% | 7.2% |
| | $T = 90$ days | 8.6% | 8.1% | 6.4% | 3.7% |
| | $T = 180$ days | 7.7% | 7.2% | 5.5% | 2.8% |

**Table 4**
Optimal vaccine allocation for each scenario and objective function. Group 1 corresponds to younger individuals (under age 65) and Group 2 corresponds to older individuals (age 65 and older).

| Objective | All scenarios No social distancing | All scenarios With social distancing |
|---|---|---|
| Minimize infections | Group 1 | Group 1 |
| Minimize deaths | Group 2 | Group 2 |
| Minimize life years lost | Group 2 | Group 2 |
| Minimize QALYs lost | Group 2 | Group 2 |

deaths, it is better to vaccinate older individuals (group 2) because their mortality rate is much higher ($\mu_2 \gg \mu_1$). Similarly for life years and QALYs lost, it is better to vaccinate older individuals (group 2), as the gain in life years and QALYs for younger individuals (group 1) is not enough to offset the higher mortality rate among older individuals.

**Sensitivity Analysis on Key Parameters.** Our estimates of COVID-19 natural history parameters are derived from several recently published studies. Because there is uncertainty around these epidemiological parameters, we examine in one-way sensitivity analysis how the optimality conditions change when varying key parameters. Across all scenarios, with and without social distancing, we find the following:

1. *Transmission rates ($\beta_{ij}$).* If $\beta_{11}$ is 1.55 times smaller, if $\beta_{22}$ is 2.18 times higher, or if $\beta_{21}$ is 1.93 times higher than our calibrated values, then it is optimal to vaccinate group 2 in order to minimize infections.
2. *Mortality rates ($\mu_i$).* As long as the mortality rate in group 2 is 1.52 times higher than in group 1, then it is optimal to vaccinate group 2 before group 1 in order to minimize deaths. We estimate in the base case that the mortality in group 2 is 38.3 times higher than in group 1, which is well above 1.52.
3. *Expected life years lost ($L_i$) and QALYs lost due to death ($q_i L_i$).* If $L_1$ is 25.1 times higher than $L_2$, then it is optimal to vaccinate group 1 before group 2 in order to minimize expected life years lost. Similarly, if $q_1 L_1$ is 25.1 times higher than $q_2 L_2$, vaccinating group 1 before group 2 minimizes QALYs lost due to death. We estimate in the base case that $L_1/L_2 = 3.5$ and $q_1 L_1/q_2 L_2 = 4.9$, values well below 25.1.

**Table 5**
Distributions for sensitivity analysis on COVID-19 transmission and natural history parameters. We denote by $x^c$ the value of parameter $x$ in the base case.

| Parameters | Distributions | |
|---|---|---|
| I(0) | U(0.01,0.1) | |
| R(0) | U(0.02,0.2) | |
| D(0) | U(0.001,0.002) | |
| $\eta$ | U(0.4, 0.95) | |
| $\beta_{ij}$ | $U(0.4\beta_{ij}^c, 1.2\beta_{i,j}^c)$ | $i,j \in [\![1,2]\!]$ |
| $\gamma_j$ | $U(0.8\gamma_j^c, 1.2\gamma_j^c)$ | $i \in [\![1,2]\!]$ |
| $\mu_j$ | $U(0.8\mu_j^c, 1.2\mu_j^c)$ | $i \in [\![1,2]\!]$ |

**Table 6**
Percentage of trials in which the approximation and the numerical simulation result in the same optimal solution for each time horizon and objective function.

| | Infections | Deaths | Life years lost | QALYs lost |
|---|---|---|---|---|
| $T = 30$ days | 86.9% | 100% | 100% | 100% |
| $T = 90$ days | 86.1% | 100% | 100% | 100% |
| $T = 180$ days | 84.9% | 100% | 100% | 100% |

### 4.3. Quality of decisions

To evaluate the accuracy of our approximated optimal allocations, we compare the above solutions to allocations determined using the exact Eqs. (1). We determine the optimal solution via exhaustive search. Since we allocate all available vaccines, we have a univariate problem in $v_2$: $(v_1, v_2) = (N/P - v_2, v_2)$. For each time horizon ($T$) and number of vaccines available ($N$), we discretize the range of feasible vaccine allocations $0 \leq v_2 \leq \min(S_1(0), S_2(0), \tau(T))$. We evaluate the objective function for each allocation, $f(N/P - v_2, v_2)$, and compare the value against $f(v_1^*, v_2^*)$, where $(v_1^*, v_2^*)$ is the approximated optimal solution. We find that in all cases (over the three time horizons and four epidemic scenarios, with and without social distancing) the approximated optimal solution is the same as the true optimal solution.

To further explore the accuracy of our approximations, we stochastically vary the transmission and natural history parameters of the model (while maintaining the 84%/16% split between groups 1 and 2). We run 8,000 trials, each time sampling the parameters from uniform distributions (Table 5). There are several vaccines against COVID, each with different effectiveness against different COVID variants. To account for this variability, we vary the vaccine effectiveness $\eta$ uniformly between 0.4 and 0.95, reflecting ranges found in the literature [42–45]. We calculate the percentage of scenarios where the approximation and numerical simulations yield the same optimal solution (Table 6). For the objectives of minimizing deaths, life years lost, and QALYs lost, the approximation and the exhaustive search with numerical simulations find the same optimal solution in every trial. For the objective of minimizing infections, the solutions match in approximately 85% of the trials.

**Sensitivity Analysis on Time Horizon.** We use numerical simulations to explore how the optimal vaccine allocation might change for a longer time horizon of two years. We find that for all four objectives, the optimal solution does not change when supplies of vaccines are limited ($v_1 + v_2 \leq \tau(T)$). For the objectives of minimizing deaths, life years lost, and QALYs lost due to death, it is still optimal to vaccinate group 2 before group 1 for any level of vaccines up to $S_1(0)$.

## 5. Discussion

In health economics, QALYs are generally used to measure health outcomes [46]. However, the appropriate objective for the vaccine allocation problem depends on the decision environment. For example, because there is currently no cure for COVID-19, policy makers may initially allocate COVID-19 vaccines to minimize deaths, as deaths are irreversible [1]. In this paper we have used an epidemic approximation to develop simple conditions characterizing the optimal vaccine allocation for four different objectives: minimize infections, deaths, life years lost, or QALYs lost due to death.

Using first- and second-order Taylor series expansions, we reduce the optimal vaccine allocation problem to a knapsack problem. If the goal is to minimize new infections (population-level health benefits), the simple conditions indicate that it is optimal to allocate vaccines to the group with the highest force of infection. If the goal is to minimize deaths (individual-level health benefits), the condition is weighted by the mortality rates; if the goal is to minimize life years or QALYs lost due to death, the condition is additionally weighted by expected life years lost or quality-adjusted expected life years lost, respectively. In all cases, if enough vaccines are available, additional vaccination of other unvaccinated groups becomes optimal, again following the simple conditions. This all-or-nothing approach is optimal for these four objective functions since the approximated problems have the same form.

Our computational results suggest that good vaccine allocation decisions can be made using these simple conditions with minimal data. For the case of COVID-19 and two interacting population groups comprising younger and older individuals, respectively, we find that it is optimal to vaccinate the younger individuals to minimize new infections. This is because the younger group is larger and is more likely to transmit the infection to older individuals than vice versa. However, if the objective is to minimize deaths, life years lost, or QALYs lost due to death, it is optimal to vaccinate the older individuals. This is because the infection fatality rate is much higher in this group. For all considered cases (varying the time horizon, epidemic scenario, with or without social distancing), the approximation yields the exact optimal solution. In stochastic sensitivity analysis, the approximated solution is optimal across all trials for the objectives of minimizing deaths, life years lost, and QALYs lost due to death, and is optimal in more than 85% of trials for the objective of minimizing new infections.

The time horizon and the objective function will depend on the specific problem setting. For COVID-19, a relatively short time horizon may be appropriate, whereas for other communicable diseases (e.g., measles) a longer time horizon might be appropriate. Our analysis is especially useful for short-term horizons, when vaccine supply may be most limited. We note that the objective may change over time: for example, policy makers may initially want to use limited vaccine supply to avert deaths in the short term and then later switch to the objective of minimizing new infections. In the case of COVID-19, government policies to initially vaccinate older individuals and healthcare workers when the vaccine supply was highly constrained are consistent with our approximated optimal solution to minimize deaths, life years lost, and QALYs lost due to death. Expansion of vaccination eligibility to younger age groups is consistent with our approximated optimal solution to minimize new infections.

Our study has several limitations. We consider a single time period with individuals vaccinated at time 0 and instantaneous vaccine effectiveness. In reality, vaccination efforts extend over time. Our analysis is based on a relatively simple SIR model. Further research could investigate whether our analytical approach could be extended to more sophisticated compartmental models that can capture more details of disease transmission and progression (e.g., age structure, quarantine, exposed individuals, asymptomatic infections or hospitalization) [47–50]. Finally, we use first- and second-order Taylor series expansions which provide reasonable approximations in the short term but might not be as accurate for longer time horizons. Future work could extend the problem to a multi-period setting.

Despite these limitations, our simple conditions provide a useful means of informing vaccine allocation decisions. As shown by our numerical simulations, the allocations resulting from these conditions match those found using much more computationally expensive algorithms such as exhaustive search, and can be used for any of the objective functions of minimizing new infections, deaths, life years lost, or QALYs lost due to death.

## Declaration of competing interest

The authors declare that they have no known competing financial interests or personal relationships that could have appeared to influence the work reported in this paper.

## Acknowledgment

This work was supported by Grant R37-DA15612 from the National Institute on Drug Abuse[http://dx.doi.org/10.13039/100000026].

## Appendix A. Supplementary data

Supplementary material related to this article can be found online at https://doi.org/10.1016/j.mbs.2021.108621.

## References

[1] National Academies of Sciences Engineering and Medicine Committee on Equitable Allocation of Vaccine for the Novel Coronavirus, Equitable Allocation of Vaccine for the Novel Coronavirus, National Academy of Sciences, Engineering and Medicine, 2020.
[2] N. Becker, D.N. Starczak, Optimal vaccination strategies for a community of households, Math. Biosci. 139 (2) (1997) 117–132.
[3] M. Tanner, L. Sattenspiel, L. Ntaimo, Finding optimal vaccination strategies under parameter uncertainty using stochastic programming, Math. Biosci. 215 (2) (2008) 144–151.
[4] S. Enayati, O. Ozaltin, Optimal influenza vaccine distribution with equity, Eur. J. Oper. Res. 283 (2) (2019) 714–725.
[5] H. Yarmand, J. Ivy, B. Denton, A. Lloyd, Optimal two-phase vaccine allocation to geographically different regions under uncertainty, Eur. J. Oper. Res. 233 (1) (2014) 208–219.
[6] H. Rodrigues, M. Monteiro, D.F.M. Torres, Vaccination models and optimal control strategies to dengue, Math. Biosci. 247 (2014) 1–12.
[7] T. Yuzo Miyaoka, S. Lenhart, J.F. Meyer, Optimal control of vaccination in a vector-borne reaction–diffusion model applied to Zika virus, J. Math. Biol. 79 (3) (2019) 1077–1104.
[8] R.M. May, R.M. Anderson, Spatial heterogeneity and the design of immunization programs, Math. Biosci. 72 (1) (1984) 83–111.
[9] G.S. Zaric, M.L. Brandeau, Resource allocation for epidemic control over short time horizons, Math. Biosci. 171 (1) (2001) 33–58.
[10] S. Mylius, T. Hagenaars, A. Lugner, J. Wallinga, Optimal allocation of pandemic influenza vaccine depends on age, risk and timing, Vaccine 26 (29–30) (2008) 3742–3749.
[11] A. Tuite, D. Fisman, J. Kwong, A. Greer, Optimal pandemic influenza vaccine allocation strategies for the Canadian population, PLoS One 5 (5) (2010) e10520.
[12] L. Matrajt, I. Longini, Optimizing vaccine allocation at different points in time during an epidemic, PLoS One 5 (11) (2010) e13767.
[13] J. Medlock, A. Galvani, Optimizing influenza vaccine distribution, Science 325 (5948) (2009) 1705–1708.
[14] A. Babus, S. Das, S. Lee, The optimal allocation of COVID-19 vaccines, in: medRxiv, Cold Spring Harbor Laboratory Press, 2020, http://dx.doi.org/10.1101/2020.07.22.20160143.
[15] L. Matrajt, J. Eaton, T. Leung, E.R. Brown, Vaccine optimization for COVID-19: who to vaccinate first?, Sci. Adv. 7 (6) (2021) eabf1374.
[16] X. Chen, M. Li, D. Simchi-Levi, T. Zhao, Allocation of COVID-19 vaccines under limited supply, in: medRxiv, Cold Spring Harbor Laboratory Press, 2020, http://dx.doi.org/10.1101/2020.08.23.20179820.
[17] New York Times, Data from The New York Times, based on reports from state and local health agencies, 2020, https://github.com/nytimes/covid-19-data.
[18] U.S. Census Bureau, National Population by Characteristics: 2010-2019, 2020, https://www.census.gov/data/tables/time-series/demo/popest/2010s-national-detail.html.
[19] Social Security Administration, Actuarial Life Table, 2016, https://www.ssa.gov/oact/STATS/table4c6.html.
[20] H. Jia, E. Lubetkin, J. Barile, W. Horner-Johnson, K. DeMichele, D. Stark, M. Zack, W. Thompson, Quality-adjusted life years (QALY) for 15 chronic conditions and combinations of conditions among US adults aged 65 and older, Med. Care 56 (8) (2018) 740–746.
[21] Q. Bi, Y. Wu, S. Mei, C. Ye, X. Zou, Z. Zhang, X. Liu, L. Wei, S.A. Truelove, T. Zhang, W. Gao, C. Cheng, X. Tang, X. Wu, Y. Wu, B. Sun, S. Huang, Y. Sun, J. Zhang, T. Ma, J. Lessler, T. Feng, Epidemiology and transmission of COVID-19 in Shenzhen China: analysis of 391 cases and 1,286 of their close contacts, Lancet Infect. Dis. 20 (8) (2020) 911–919.
[22] S.A. Lauer, K.H. Grantz, Q. Bi, F.K. Jones, Q. Zheng, H. Meredith, A.S. Azman, N.G. Reich, J. Lessler, The incubation period of COVID-19 from publicly reported confirmed cases: estimation and application, Ann. Intern. Med. 172 (9) (2020) 577–582.
[23] A. Hill, Modeling COVID-19 Spread vs Healthcare Capacity, 2020, https://alhill.shinyapps.io/COVID19seir/.
[24] S. Sanche, Y.T. Lin, C. Xu, E. Romero-Severson, N. Hengartner, R. Ke, The novel coronavirus, 2019-nCoV, is highly contagious and more infectious than initially estimated, in: medRxiv, Cold Spring Harbor Laboratory Press, 2020, https://www.medrxiv.org/content/early/2020/02/11/2020.02.07.20021154.
[25] F. Zhou, T. Yu, R. Du, G. Fan, Y. Liu, Z. Liu, J. Xiang, Y. Wang, B. Song, X. Gu, L. Guan, Y. Wei, H. Li, X. Wu, J. Xu, S. Tu, Y. Zhang, H. Chen, B. Cao, Clinical course and risk factors for mortality of adult inpatients with COVID-19 in Wuhan, China: a retrospective cohort study, Lancet 395 (102229) (2020) 1054–1062.
[26] Z. Wu, J.M. McGoogan, Characteristics of and important lessons from the coronavirus disease 2019 (COVID-19) outbreak in China: summary of a report of 72,314 cases from the Chinese Center for Disease Control and Prevention, JAMA 323 (13) (2020) 1239–1242.
[27] R. Verity, L.C. Okell, I. Dorigatti, P. Winskill, C. Whittaker, N. Imai, G. Cuomo-Dannenburg, H. Thompson, P. Walker, H. Fu, A. Dighe, J. Griffin, M. Baguelin, S. Bhatia, A. Boonyasiri, A. Cori, Z. Cucunuba, R. FitzJohn, K. Gaythorpe, W. Green, A. Hamlet, W. Hinsley, D. Laydon, G. Nedjati-Gilani, S. Riley, S. van Elsland, E. Volz, H. Wang, Y. Wang, X. Xi, C. Donnelly, A. Ghani, N.M. Ferguson, Estimates of the severity of coronavirus disease 2019: a model-based analysis, Lancet Infect. Dis. 20 (6) (2020) 669–677.
[28] A.T. Levin, W.P. Hanage, N. Owusu-Boaitey, K.B. Cochran, S.P. Walsh, G. Meyerowitz-Katz, Assessing the age specificity of infection fatality rates for COVID-19: systematic review, meta-analysis, and public policy implications, Eur. J. Epidemiol. 35 (12) (2020) 1123–1138.
[29] M. Thompson, J. Burgess, A. Naleway, et al., Interim estimates of vaccine effectiveness of BNT162b2 and mRNA-1273 COVID-19 vaccines in preventing SARS-CoV-2 infection among health care personnel, first responders, and other essential and frontline workers — eight U.S. locations, december 2020–march 2021, Morb. Mortal Wkly. Rep. 70 (13) (2021) 495–500.
[30] R. Li, S. Pei, B. Chen, Y. Song, T. Zhang, W. Yang, J. Shaman, Substantial undocumented infection facilitates the rapid dissemination of novel coronavirus (SARS-CoV-2), Science 368 (6490) (2020) 489–493.
[31] D. Sutton, K. Fuchs, M. D'Alton, D. Goffman, Universal screening for SARS-CoV-2 in women admitted for delivery, New Engl. J. Med. 382 (22) (2020) 2163–2164,
[32] Official New York State Portal, New York State on PAUSE, 2020, Washington Post, coronavirus.health.ny.gov/new-york-state-pause.
[33] M. Mckay, R.J. Beckman, W.J. Conover, A comparison of three methods for selecting values of input variables in the analysis of output from a computer code, Technometrics 42 (1) (2000) 55–61.
[34] S. Sanche, Y. Lin, C. Xu, E. Romero-Severson, N. Hengartner, R. Ke, High contagiousness and rapid spread of severe acute respiratory syndrome coronavirus 2, Emerg. Infect. Dis. 26 (7) (2020) 1470–1477.
[35] A.R. Ives, C. Bozzuto, Estimating and explaining the spread of COVID-19 at the county level in the USA, Commun. Biol. 4 (60) (2021).
[36] B. Tang, X. Wang, Q. Li, N.L. Bragazzi, S. Tang, Y. Xiao, J. Wu, Estimation of the transmission risk of the 2019-nCoV and its implication for public health interventions, J. Clin. Med. 9 (2) (2020) 462.
[37] R. Subramanian, Q. He, M. Pascual, Quantifying asymptomatic infection and transmission of COVID-19 in New York City using observed cases, serology, and testing capacity, Proc. Nat. Acad. Sci. USA 118 (9) (2021) e2019716118.
[38] United States Coronavirus (COVID-19) tracker, 2020, [Online]. Available: https://infection2020.com/.
[39] S. Anand, M. Montez-Rath, J. Han, J. Bozeman, R. Kerschmann, P. Beyer, J. Parsonnet, G.M. Chertow, Prevalence of SARS-CoV-2 antibodies in a large nationwide sample of patients on dialysis in the USA: a cross-sectional study, Lancet 396 (10259) (2020) 1335–1344.
[40] E. Del Fava, J. Cimentada, D. Perrotta, A. Grow, F. Rampazzo, S. Gil-Clavel, E. Zagheni, The differential impact of physical distancing strategies on social contacts relevant for the spread of COVID-19, in: medRxiv, Cold Spring Harbor Laboratory Press, 2020, http://dx.doi.org/10.1101/2020.05.15.20102657, https://www.medrxiv.org/content/10.1101/2020.05.15.20102657v1.
[41] N. Jones, C. Carver, Are interventions such as social distancing effective at reducing the risk of asymptomatic healthcare workers transmitting COVID-19 infection to other household members?, Centre for Evidence-Based Medicine, University of Oxford, 2020, https://www.cebm.net/covid-19/are-interventions-such-as-social-distancing-effective-at-reducing-the-risk-of-asymptomatic-healthcare-workers-transmitting-covid-19-infection-to-other-household-members/.
[42] K. Emary, T. Golubchik, P. Aley, C. Ariani, B. Angus, S. Bibi, B. Blane, D. Bonsall, P. Cicconi, S. Charlton, E. Clutterbuck, A. Collins, T. Cox, T. Darton, C. Dold, A. Douglas, C. Duncan, K. Ewer, A. Flaxman, D. O'Connor, Efficacy of ChAdOx1 nCoV-19 (AZD1222) vaccine against SARS-CoV-2 variant of concern 202012/01 (B.1.1.7): an exploratory analysis of a randomised controlled trial, Lancet 397 (10282) (2021) 1351–1362.
[43] Pfizer and BioNTech confirm high efficacy and no serious safety concerns through up to six months following second dose in updated topline analysis of landmark COVID-19 vaccine study, Bus. Wire (2021) [Online]. Available: https://www.businesswire.com/news/home/20210401005365/en/.

[44] F.P. Polack, S.J. Thomas, N. Kitchin, J. Absalon, A. Gurtman, S. Lockhart, J.L. Perez, G. Pérez Marc, E.D. Moreira, C. Zerbini, R. Bailey, K.A. Swanson, S. Roychoudhury, K. Koury, P. Li, W.V. Kalina, D. Cooper, R.W. Frenck, L.L. Hammitt, O. Tureci, H. Nell, A. Schaefer, S. Unal, D.B. Tresnan, S. Mather, P.R. Dormitzer, U. Sahin, K.U. Jansen, W.C. Gruber, Safety and efficacy of the BNT162b2 mRNA COVID-19 vaccine, New Engl. J. Med. 383 (27) (2020) 2603–2615.

[45] E. Mahase, COVID-19: Moderna vaccine is nearly 95% effective, trial involving high risk and elderly people shows, BMJ 371 (2020) m4471.

[46] P.J. Neumann, G.D. Sanders, L.B. Russell, J.E. Siegel, T.G. Ganiats, Cost-effectiveness in health and medicine, 2nd edition, Oxford University Press, New York, 2016.

[47] C.N. Ngonghala, E. Iboi, S. Eikenberry, M. Scotch, C.R. MacIntyre, M.H. Bonds, A.B. Gumel, Mathematical assessment of the impact of non-pharmaceutical interventions on curtailing the 2019 novel coronavirus, Math. Biosci. 325 (2020) 108364.

[48] Q. Li, B. Tang, N.L. Bragazzi, Y. Xiao, J. Wu, Modeling the impact of mass influenza vaccination and public health interventions on COVID-19 epidemics with limited detection capability, Math. Biosci. 325 (2020) 108378.

[49] M.A. Acuna-Zegarra, M. Santana-Cibrian, J.X. Velasco-Hernandez, Modeling behavioral change and COVID-19 containment in Mexico: a trade-off between lockdown and compliance, Math. Biosci. 325 (2020) 108370.

[50] R. Stutt, R. Retkute, M. Bradley, C. Gilligan, J. Colvin, A modelling framework to assess the likely effectiveness of facemasks in combination with 'lock-down' in managing the COVID-19 pandemic, Proc. R. Soc. Lond. Ser. A Math. Phys. Eng. Sci. 476 (2238) (2020) 20200376.